Failure and post-failure analysis of submarine mass movements using geomorphology and geomechanical concepts

JACQUES LOCAT

Laboratoire d'études sur les risques naturels, Department of Geology and Geological Engineering, Laval University, Québec, Canada, G1V 0A6

jacques.locat@ggl.ulavcal.ca

Abstract: Access to submarine slopes is usually limited and it is often difficult to rely on deep cores or *in situ* measurements to determine the geotechnical characteristics of the sediments involved in a slide when carrying out back-analyses of submarine mass movements and their consequences. The approach presented here uses geomorphology and basic geomechanical concepts to reduce uncertainties in slope stability and mobility analyses. It shows how geomorphology can be used to select the geomechanical input parameters required in failure and post-failure analyses. Typical parameters derived from such analyses are related to the strength of the material, the pore water pressure at the time of failure, and the rheological properties of post-failure debris or mud flows.

Access to submarine slopes for geotechnical investigations is often limited to major projects, such as gas development along the Storegga Escarpment (Kvalstad *et al.* 2005), or to investigations that can rely on *in situ* measurements (Sultan *et al.* 2007*a*, *b*). In most studies the analysis can only be based on multibeam imagery (Mosher & Piper 2007), seismic (two- or three-dimensional) surveys and shallow gravity cores, which can be of variable quality and length depending on the amount of gas present in the pore water and the type of sampler used. To compensate, investigations have often relied on basic soil mechanics concepts (Poulos 1988), as shown by the studies of Lee & Edwards (1986) and Lee *et al.* (1991) for the slope off California, which took into account the relationships between soil strength and depth. Taking advantage of high-resolution multibeam seismic surveys, experience was gained linking the morphology of a slope to geomechanical (i.e. soil and fluid mechanics) concepts applicable to either the failure or post-failure analysis of mass movements. It may be difficult to resolve the morphology of shallow slopes at great depths (>1000 m) using multibeam bathymetry data obtained from sources near the surface of the sea. This has been resolved by using an autonomous underwater vehicle carrying a multibeam system at great depth and keeping it <100 m above the seafloor, which resulted in excellent resolution (Locat 2017). This approach is mostly limited to sediments (or soils in the engineering sense) because it does not consider the potential role of the discontinuities seen in most mass movements involving rocks. In addition, and in particular for the post-failure analysis, a clear identification of both the source and depositional morphology of a given mass movement is necessary.

This paper mainly considers slides and debris flows and, to some extent, debris avalanches (Hungr *et al.* 2013; Locat 2017). The approach developed via various case studies is presented as follows: a review of geomechanical concepts; the classification of slopes; the strength of eroded slopes (intact strength); and the strength of debris and mud flow deposits (remoulded strength) at the time of deposition. Examples are provided to illustrate this approach. This paper will help our understanding of both the nature of some slide deposits and the conditions prevailing at failure, as well as helping to structure the back-analysis of mass movements (failure and post-failure). For more in-depth geotechnical aspects dealing with submarine slope instabilities, readers are referred to Sultan *et al.* (2004*a*, *b*, 2007*a*, *b*) and Lee *et al.* (2007).

Geomechanical concepts

The main geomechanical concepts related to slope formation involve the basic principles relating the morphology of a slope (slope height, slope angle, thickness of the debris deposit and the slope of the slide debris) to the strength both before (soil mechanics) and after (fluid mechanics) failure. The concepts considered in this paper are limited to sediment formation and strength, the factor of safety and stability analysis, and the yield strength and mobility. More details of these concepts are presented in Lee *et al.* (2007).

From: Lintern, D. G., Mosher, D. C., Moscardelli, L. G., Bobrowsky, P. T., Campbell, C., Chaytor, J. D., Clague, J. J., Georgiopoulou, A., Lajeunesse, P., Normandeau, A., Piper, D. J. W., Scherwath, M., Stacey, C. & Turmel, D. (eds) *Subaqueous Mass Movements*. Geological Society, London, Special Publications, **477**,
https://doi.org/10.1144/SP477.27

Sediment formation and strength

A conceptual approach to sediment formation and strength is shown in Figure 1. It considers four aspects: (1) the depositional environment; (2) the formation and evolution of the sediment; (3) the energy available at the time of a slide event; and (4) the possible failure mechanisms. The relevant physical properties related to these four aspects are also shown in Figure 1.

Depositional environment. The depositional environment determines whether sediments are stratified or homogeneous. Stratified sediments are characterized by changes in texture. The nature of the sediment also affects its behaviour. Most of the soil mechanics concepts presented here were developed for inorganic soils (Poulos 1988). Other types of sediments, such as fossiliferous sediments (mostly foram- and diatom-rich sediments), have also been studied and their properties show some differences from those of classical soil mechanics based on inorganic sediments (Pittenger *et al.* 1989; Rack *et al.* 1993; Tanaka & Locat 1999; Locat & Tanaka 2001; Shiwakoti *et al.* 2002; Locat *et al.* 2003; Lee *et al.* 2011; Wiemer & Kopf 2017). Other features of the development of large landslides, including the effects of pore pressure, have been reported by Talling *et al.* (2014), whereas the impact of gas on landslide development has been illustrated by Saint-Ange *et al.* (2014) for the Beaufort Sea area and Bünz *et al.* (2005) for the Storegga Slide. The formation of gas hydrates and their effects on the stability of submarine slopes have been reviewed by Mienert *et al.* (2005) and Grozic (2010).

Because the marine environment favours deposition over large areas and records many geological changes from either land or marine sources, stratified deposits are the most frequent style of deposition. Clinoforms can develop over large areas, generating potential marker horizons that may be involved in generating large mass movements. Example of these can be found in the North Sea (e.g. the Storegga Slide, Kvalstad *et al.* 2005), the shelf and continental

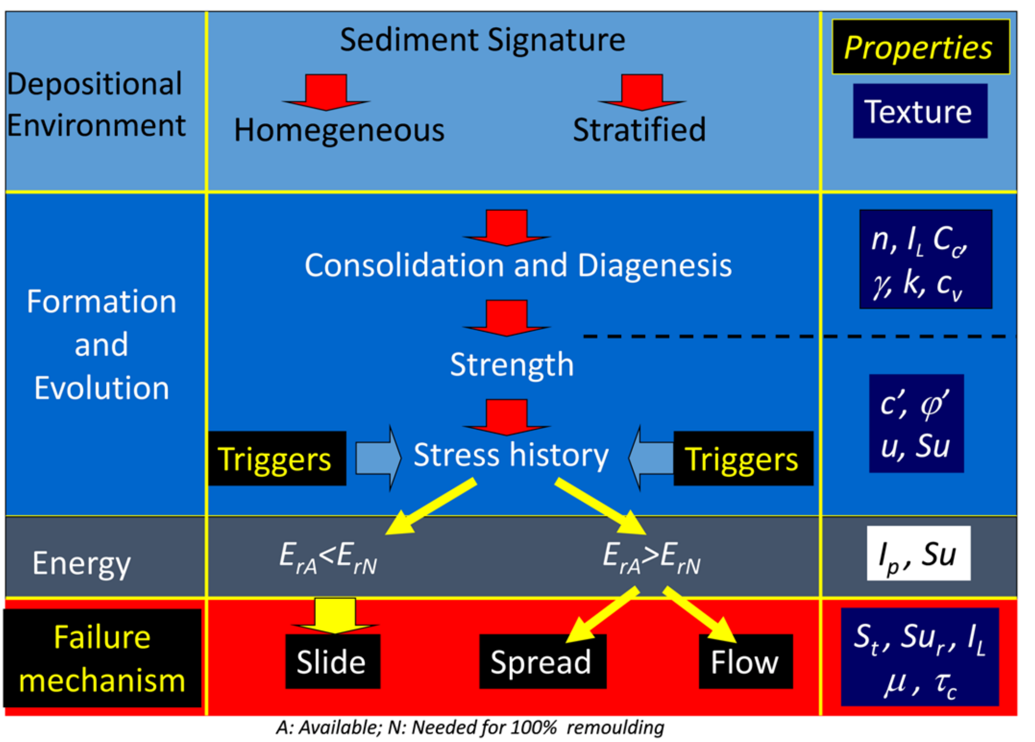

Fig. 1. Processes from sediment deposition to failure; see text for explanation. The physical properties considered here are: porosity (n), specific unit weight (γ), compression index (C_c), coefficient of volumetric consolidation (c_v), hydraulic conductivity (k), cohesion (c'), friction angle (ϕ'), pore pressure (u), undrained shear strength (Su), plasticity index (I_p), sensitivity (S_t), liquidity index (I_L), viscosity (μ) and yield strength (τ_c). The energy here is the energy related to remoulding (Leroueil *et al.* 1996): E_{rA}, energy available for remoulding; E_{rN}, energy necessary for 100% remoulding.

slope of the Gulf of Lion (Baztan *et al.* 2005), and the Atlantic continental slope of Canada and the USA (Brothers *et al.* 2013). A system favouring the development of layers of different grain sizes can also provide conditions for the development of potential or active weak layers (Locat *et al.* 2014).

Sediment formation and shear strength. Following deposition, sediments experience a number of different processes as a result of burial, including consolidation and diagenesis (Poulos 1988). Cementation may develop and strength may be gained via seismic strengthening (Lee *et al.* 2004, 2007; Sawyer & DeVore 2015; ten Brink *et al.* 2016).

As the accumulation of sediment increases, the sediment particles are buried under an increasing weight of sediments, which can give rise to excess pore water pressures that must be expelled from the soil structure so that the sediment can adjust to the increasing weight through the process of consolidation (Gibson *et al.* 1967, 1981). In most cases the sedimentation rate is sufficiently low that there is enough time for the dissipation of excess pore pressure and the sediment becomes normally consolidated, i.e. the consolidation strength (σ'_p) is equal to the effective stress (σ'_{vo}). In this case, the ratio of undrained shear strength (Su) to the vertical effective stress will vary between 0.2 and 0.4 (Poulos 1988). An excellent example of a normally consolidated sediment is the inorganic clays of the Gulf of Mexico (Quiros *et al.* 1983) (Fig. 2). This is a rare example where *in situ* measurements are available

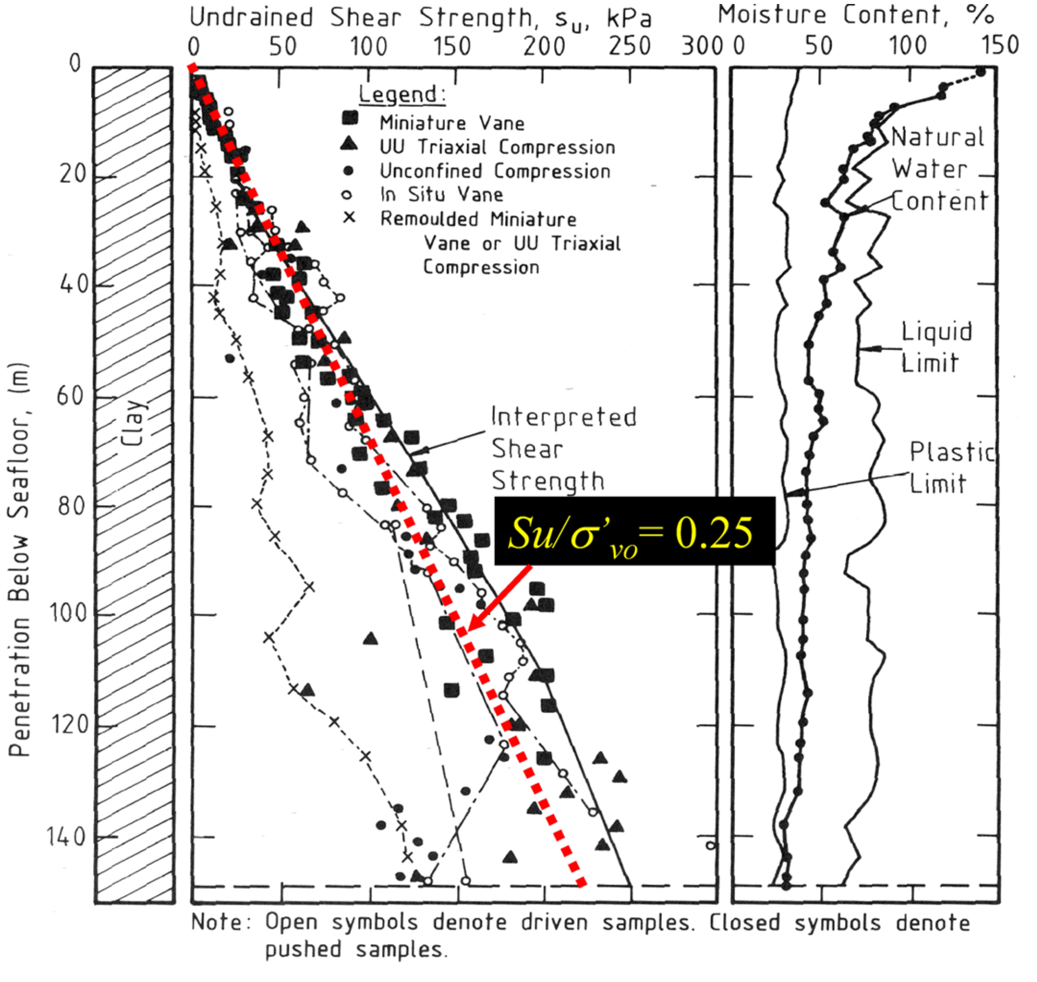

Fig. 2. Example of the profile of a normally consolidated sediment taken from the Gulf of Mexico area. This profile provides both intact and remoulded strength measurements on cores and the *in situ* strength measured with a field vane. The theoretical relationship Su/σ'_{vo} has been added (red dashed line) for comparison (modified after Quiros *et al.* 1983 in Poulos 1988).

down to a depth of 140 m. This geotechnical profile also shows a decreasing water content, equivalent to a decrease in the liquidity index I_L, where $I_L = (w - w_P)/(w_L - w_P)$ and w, w_P and w_L are, respectively, the water content and the plastic and liquid limits of the sediment, all expressed as a percentage by weight. If there is evidence for a normally consolidated or an over-consolidated sediment (i.e. a sediment for which $\sigma'_p > \sigma'_{vo}$), this indicates that, if significant pore pressures (or their equivalent) exist in the sediment, they were probably generated after the end of the consolidation process of the normally consolidated or over-consolidated stratigraphic sequence. In such a case, the sedimentation rates associated with the formation of the stratigraphic sequence cannot explain the presence of the excess pore water pressures. A recent rapid depositional event could temporarily generate excess pore pressures as part of a sedimentation/consolidation process, but its effects in terms of pore pressure will also vanish with time.

If erosion takes place in part of a slope that was formed by a normally consolidated sediment, then this part of the slope will become over-consolidated, as seen in the Point-du-Fort submarine slide (Locat *et al.* 2018) (Fig. 3). In rare examples, such as the Mississippi delta, the sedimentation rate is faster than the rate at which the sediments can fully consolidate (Shephard *et al.* 1978). In this region, Prior & Suhayada (1979) reported a pore pressure ratio as high as 0.986, indicative of little consolidation and characteristic of a very soft, unconsolidated sediment ($\sigma'_p < \sigma'_{vo}$). Similar observations were made offshore the Gulf of Mexico by Flemings *et al.* (2008). The pore pressure ratio for subaqueous conditions r_u^+ is equal to $u^+/\gamma' H^*$, where u^+ is the excess pore water pressure (i.e. in addition to the hydrostatic pressure; Poulos 1988) and H^* is the height of the slice above the rupture surface considered in the stability analysis. Because the sediment is below sea-level, the buoyant unit weight (γ') is used to calculate the pore pressure ratio. The buoyant unit weight is also called the submerged unit weight, so that $\gamma' = \gamma_{sat} - \gamma_w$, where γ_{sat} is the saturated unit weight of the sediment and γ_w is the unit weight of water. Two points should be noted. First, the use of ‘unconsolidated’ to describe sediments (or soils) rather than rocks should be avoided and replaced by the term ‘non-indurated’ if sediments (or soils) are compared with rocks. Second, the consolidation processes are nearly irreversible, i.e. once the void ratio of a sediment has decreased with increasing pressure (stress), any future reduction in effective stress due to erosion or an increase in pore pressure will not be able to increase the water content or the porosity, except for limited swelling in some situations, such as unloading by erosion.

As the sediment develops its strength, it will also acquire an intact undrained shear strength (Su), which will be greater than the remoulded undrained shear strength (Su_r), and the ratio of these two strengths is called the sensitivity ($S_t = Su/Su_r$). The sensitivity of marine sediments varies between 5 and 10 in most instances (Perret *et al.* 1995), but

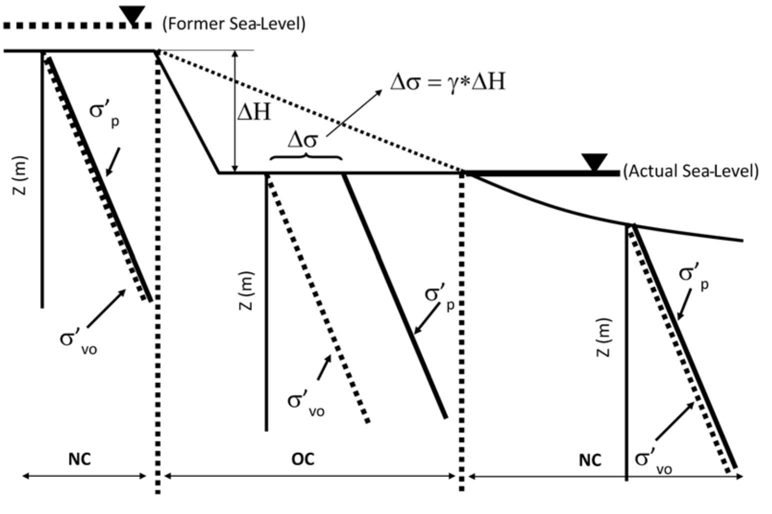

Fig. 3. Effect of sea-level change and erosion on the coastal profile in the Baie des Ha! Ha! (Saguenay Fjord) at the location of the Point-du-Fort Slide. The actual tidal flat, at sea-level, represents erosion (ΔH) of *c.* 15 m generating an over-consolidated deposit, i.e. the consolidation pressure (σ'_p) is greater than the *in situ* effective stress (σ'_{vo}). Above and below the eroded part of the slope, the sediment is normally consolidated. The slide was initiated from the shoreline and into the fjord (Locat *et al.* 2007). NC, normally consolidated deposit; OC, over-consolidated deposit.

can reach values >100 in marine sediments that have been leached to a low salinity (often <2 g l^{-1}), substantially affecting their index properties (Longva *et al.* 2003).

Energy and failure mechanisms. Depending on the sediment strength, the energy available at the time of the slide event and the existing pore pressure, the development of a spread or a flow slide may depend on the capacity of the sediment to be partially or totally remoulded. Rotational or translational slides can be evaluated using standard slope stability procedures, but these cannot be used for flows or spreads.

In the case of a flow slide, the material must be remoulded to such a degree that the failed mass can flow out of the rupture surface. The available remoulding energy (E_{rA}) is then close to, or greater than, the energy required (E_{rN}) to reach 100% of the remoulded undrained shear strength of the sediment, or must be sufficient to generate a volume of remoulded material that can transport the remaining mass of debris, such as in 'flake slides' or translational progressive landslides (Hungr *et al.* 2013). This is often seen for slides in sensitive clays (Thakur *et al.* 2014) or if failure by liquefaction occurs as a result of an earthquake (Levesque *et al.* 2006).

Two major characteristics are needed for a spread failure to take place: a strain-softening material and a stress change to trigger it, such as a first slide (Hungr *et al.* 2013). The rupture surface is developed via a progressive failure mechanism (Locat *et al.* 2011; Leroueil *et al.* 2012). If the geometric conditions favour the evacuation of the slide debris after a spread failure, part of the material may transform into a flow slide (e.g. the Storegga Slide, Kvalstad *et al.* 2005).

Factors of safety and stability analysis

The factor of safety of a slope, from a limit equilibrium analysis, is the amount of reduction in the strength (resisting forces) necessary to bring the soil to a state of equilibrium with the driving forces, i.e. when the resisting forces are equal to the gravitational forces. This concept is limited to slides and is not directly applicable to flow slides or spreads. In general, the factor of safety is equal or greater than unity:

$$\text{Factor of safety} = \frac{\sum \text{Resisting forces}}{\sum \text{Driving forces}} \geq 1 \qquad (1)$$

Here it is considered that the resisting force of the sediment follows a Mohr–Coulomb failure criterion such as:

$$\tau = c' + \sigma' \tan(\varphi') \qquad (2)$$

where τ is the shearing resistance, c' is the cohesion, σ' is the effective stress if we consider that hydrostatic conditions exist below sea-level (i.e. using the buoyant weight γ') and φ' is the friction angle. The friction angle is usually determined using triaxial tests, but a crude relationship has been established between the friction angle and the plasticity index, I_p, which is mostly applicable to non-fossiliferous sediments (Locat & Tanaka 2001). The cohesion is also determined using triaxial tests, but is very sensitive to remoulding. For illitic marine clays, such as post-glacial sediments in eastern Canada, we can use a cohesion value of *c.* 8 kPa in the absence of direct measurements of cohesion (Lefebvre 1981).

In some cases, we can rewrite equation (2) using the pore pressure ratio for subaqueous conditions (r_u^+). In this case, equation (2) becomes:

$$\tau = c' + \sigma'(1 - r_u^+) \tan(\varphi') \qquad (3)$$

Here, $(1 - r_u^+)\tan(\varphi')$ can be regarded as an apparent, or mobilized, friction angle because the friction angle is considered to be constant. Note that, compared with subaerial slope conditions, the same excess pore pressure u^+ for underwater conditions will generate a higher pore pressure ratio in the sediment because it will be applied on the buoyant unit weight γ'.

For natural slopes, Locat *et al.* (2000) and Locat (2001) proposed that over long periods of time (including geological timescales), the slope angle reflects the equilibrium between the characteristics (and strength) of the soil or rock and the processes leading to its formation, i.e. it can be assumed that for a natural slope the long-term factor of safety of a slope is close to unity. This is similar to the 'angle of ultimate stability' of Hutchinson (2001), which he considers to be a basic unit of the landscape, with values close to the residual friction angle (for soils). Here, this concept is applied to eroded slopes. Figure 4 illustrates this general concept, i.e. that if a slope is being actively eroded, the factor of safely is probably around unity, whereas if changes in the morphology take place, the factor of safety can either decrease or increase depending on the evolution of the erosion process and other factors such as earthquakes. Figure 4b uses the morphology of the Hudson Canyon and nearby canyons to illustrate this. This method shows that the Hudson Canyon is active with a factor of safety value close to unity for bordering slopes, whereas two other canyons have been (or are) filled, suggesting an increase in the factor of safety for these latter slopes.

Another method used to illustrate the strength of an existing slope is to consider the relationship between the slope height and the slope angle at

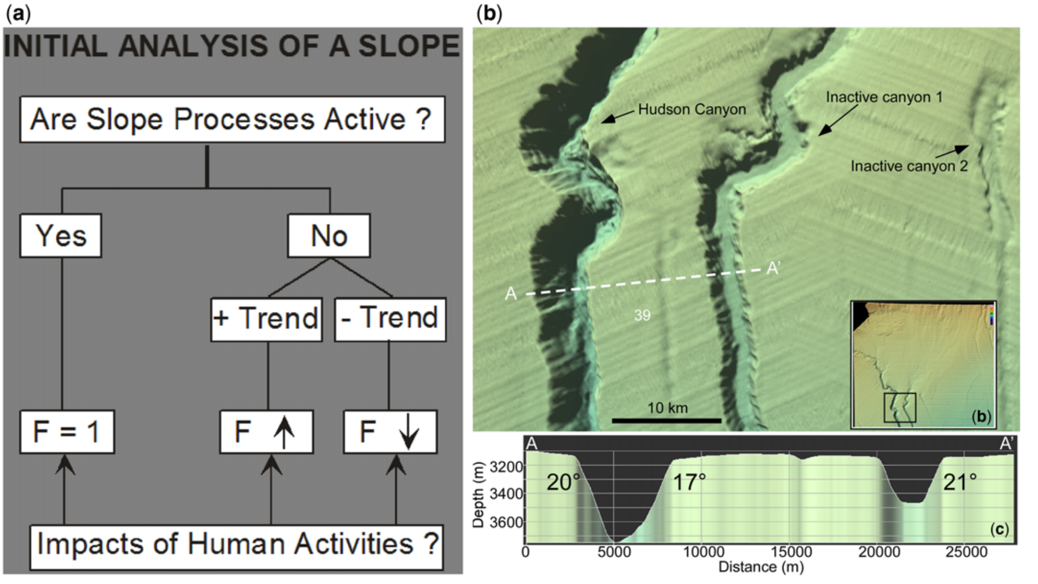

Fig. 4. (**a**) Evolution of the factor of safety of a slope (F). (**b**) Example of active and inactive canyons and the potential effect of slope stability where canyon filling can be seen as a process increasing the factor of safety of the slope. Average slope angles are given on the cross-section.

equilibrium (i.e. for FS = 1). A computation using Slope/*W* software has been carried out for a slope in homogeneous sediments consisting of a normally consolidated clay. The analysis was performed for both drained and undrained conditions. The drained example corresponds to a scenario in which the sliding process takes place so slowly that no significant excess pore water pressure develops as part of the slide-triggering mechanism. In this case, the strength parameters used are c' and φ'. For the undrained example, it is assumed that the destabilizing process is rapid enough to mobilize the undrained shear strength of the sediments. In this case, undrained shear strength *Su* is used. The results of this parametric analysis are presented in Figure 5 where, in all cases, the rupture surface is forced to exit near the toe of the slope.

For the drained case with no excess pore pressure and a slope at equilibrium, the height (H) of the slope will tend to infinity if the slope angle approaches the friction angle. Once the slope height reaches >100 m for sediments (not for rocks), the portion of the shearing resistance due to cohesion becomes negligible (Locat *et al.* 2009) and the equilibrium slope angle quickly tends towards a value equal to the friction angle, i.e. 30°. With respect to cohesion, Ikari & Kopf (2011) concluded that their experiments showed that some gain in cohesion with burial depth is possible, but they did not explain why their (smectite-rich) samples did not exhibit swelling behaviour after unloading, which is contrary to the expected behaviour of most clayey soils and of swelling clays in particular (Mesri *et al.* 1978). Figure 5 also shows that if there is enough time for an erosion process to take place, then it can generate high slopes if the area is fairly quiet seismically. However, if large earthquakes are frequent, such as along active margins, it may be difficult to generate very large landslides by the process of erosion because the earthquakes will prevent the development of very high slopes by erosion only. For a rotational slide to take place on a steep slope (i.e. >40°), the rupture surface needs to be near to the toe of the slope (Steward *et al.* 2011).

As some seepage forces may exist in submarine slopes (e.g. Flemings *et al.* 2008), or equivalent excess pore pressures due to the dissociation of gas hydrates (e.g. Riboulot *et al.* 2013; Saint-Ange *et al.* 2014), drained analysis with excess pore pressures (i.e. above hydrostatic) can also be considered by using the r_u^+ parameter in the computation. As expected, the relationship between the slope height and the slope angle gives values for the angle that are always below the value of the friction angle of the sediment, i.e. 30° in the example shown in Figure 5. This figure shows that as excess pore pressure build ups in a sedimentary sequence or along certain stratigraphic horizons, the equilibrium slope angle will decrease with increasing r_u^+.

For the undrained case, the critical slope angle remains at 15° for any height as long as the strength to stress ratio remains constant with depth (here

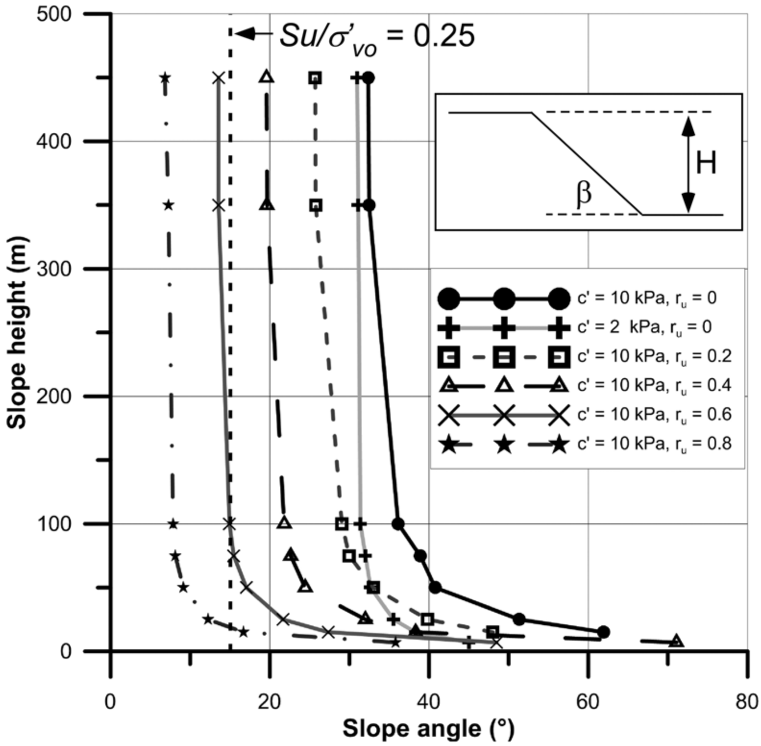

Fig. 5. Analysis of a homogeneous slope in clay using the Slope/*W* software to illustrate the relationship between slope height (H) and slope angle (β) for FS = 1, for both drained and undrained examples and for a rupture surface exiting at the toe of the slope. For the drained example, the properties used for the analysis are: $\phi' = 30°$, $c' = 10$ and 2 kPa, and $\gamma' = 10$ kN m^{-3}. In addition, r_u^+ values of 0.2 (24.8°), 0.4 (19.2°), 0.6 (13.1°) and 0.8 (6.6°) are shown using $\phi' = 30°$ and $c' = 10$ kPa. Values in parentheses give the equivalent mobilized friction angle. For the undrained example, a value of $Su/\sigma'_{vo} = 0.25$ is used. Note that this graph is for illustration purposes only and cannot be used for the evaluation of stability.

$Su/\sigma'_{vo} = 0.25$) (Fig. 5). This suggests that if a clay slope of any height, but with a slope angle >15°, is exposed after a drained failure, it could be unstable until the slope angle reaches a value of ≤15° (assuming $Su/\sigma'_{vo} = 0.25$). This may be seen as a simplified illustration for the initiation of a retrogressive failure process if the resulting new slopes remain unstable in an undrained mode until stabilization conditions are met.

Yield strength and mobility

Because the first failure of a slope may result in either a flow slide (debris or mud flow) or a spread, some transformation of the failed mass is necessary up to the point at which it behaves as a fluid. We could consider such a mixture from a soil mechanics point of view, but then we would have to consider high excess pore pressures that would not have enough time to dissipate significantly due to the short duration of the flow event relative to the time for required for the dissipation of significant amounts of excess pore pressure (Locat *et al.* 1996). This is why flow slides are generally modelled as a fluid. Using an example of debris flows on the Mississippi Fan (Schwab *et al.* 1996), Locat *et al.* (1996) estimated that for a 2–3 m thick single flow event, only *c.* 1% of the excess pore pressure would have had time to dissipate after one day. To that effect, for coarser flow slides, a soil mechanics approach using a slide consolidation model has been able to reproduce the observed velocities by calculating the dissipation of excess pore pressure at the base of the flow slide (Hutchinson 1986; Qiao & Clayton 2013). The link between soils and fluid mechanics for flow slides may be seen by the fact that the remoulded undrained shear strength (soil mechanics) of a sediment is nearly equivalent to its yield strength (fluid mechanics; Locat & Demers 1988).

In general, the rheological characteristics of a viscous fluid are described by its yield strength (τ_c) and viscosity (μ) (Locat & Demers 1988; Coussot & Piau

1994; Locat 1997; Malet *et al.* 2002; Jeong *et al.* 2010). It is then necessary to use rheological models to describe the flow behaviour of such a mixture to provide some input for modelling the mobility of these flows; these models can also be used to model tsunami (Grilli *et al.* 2017). A common piece of software used for such an analysis is BING, which can use a number of different rheological models, such as the Bingham, Herschel–Bulkley and bilinear models (Imran *et al.* 2001).

In many cases, the mobilized (field) yield strength is often related to the back-calculated value obtained using the concept of the critical thickness (H_c) (Hampton 1972), which considers that, everything being equal, there is a maximum thickness below which the flow will stop on a given slope angle. This relationship is expressed as:

$$H_c = \left(\frac{\tau_c}{\gamma' \sin \beta} \right) \tag{4}$$

where τ_c is the yield strength of the sediment, γ' is the buoyant unit weight and β is the angle of the slope over which the flow comes to rest. This equation is equivalent to that used for infinite slope stability analysis for a remoulded sediment.

The yield strength of a sediment can also be determined in the laboratory. Locat & Demers (1988) have shown that the yield strength can also be predicted, as a first approximation, by the remoulded undrained shear strength, i.e. $Su_r \cong \tau_c$. There are also relationships directly linking the liquidity index (I_L) to Su_r and then to τ_c (Locat & Demers 1988). Locat & Lee (2005) presented these relationships in a general form:

$$\tau_c = \left[\frac{a}{I_L} \right]^b \tag{5}$$

$$\mu = \left[\frac{c}{I_L} \right]^d \tag{6}$$

Parameters *a* and *d* in these relationships are not constant values and must be determined by rheological and physical tests on sediments. For post-glacial marine clays in Québec, the values of parameters *a*, *b*, *c*, and *d* are 12, 3, 9 and 3, respectively (Locat & Lee 2005).

These relationships show that for a given slope generating a debris or mud flow deposit, it is possible to make a first estimation of the yield strength of the flow slide responsible for depositing that layer. The only condition that could prevent the direct use of this relationship would be if hydroplaning (Mohrig *et al.* 1998) or wetting could take place during the flow (De Blasio *et al.* 2005).

For debris flows containing clayey clasts, Locat & Lee (2002), using the approach of Hampton (1975), have shown that if the water content of the clasts has not changed since deposition, or if it can be estimated, then the rheological conditions under which the flow took place can be estimated. For this to be applicable, the water content of the matrix must have remained greater than that of the clast.

In practice, Locat & Demers (1988) have shown that the contribution of the viscosity to the overall flow shearing resistance of a mud is *c.* 1 : 1000, so that in many instances the role of the viscosity is negligible for clayey flows. Jeong *et al.* (2010) observed that the ratio decreases to 1 : 100 for sandy mixtures.

The mobility of a failed mass will depend on many factors, including the volume, the rate of change in the shear strength from the peak to remoulded conditions, and the slope over which the flow takes place. The mobility can be analysed using two-dimensional (e.g. BING; Imran *et al.* 2001) or three-dimensional (e.g. OpenFOAM; Turmel *et al.* 2017) flow models, which require input parameters such as the yield strength and viscosity. A parametric analysis can be performed using such models that can relate the volume, yield strength, run-out distance and shape of the final deposit (including the thickness). In addition to this approach, many empirical relationships have been proposed to relate the volume of the displaced mass to the run-out distance to determine the mobility of landslide debris (Edgers & Karlsrud 1982; Locat & Lee 2002; Issler *et al.* 2005); these are of interest because they can help us to determine whether the mass flow deposit is the result of a single slide event.

Types of slope for which the strength can be estimated

Submarine (or subaerial) slopes can result from various geological processes. They can be categorized in terms of the slope process to help identify those for which it may be possible to estimate the strength of the material at the time of formation. Slopes can be grouped into a minimum of four types of formation processes: (1) sedimentation/accumulation; (2) erosion; (3) tectonism; and (4) volcanism (Fig. 6). Slopes generated by sedimentation/accumulation can result from the formation of clinoforms (type 1a), which is a dominant process on many margins, the accumulation of mud or debris flows (1b), turbidites (type 1c) or biogenic processes (1d). Eroded slopes can result from direct erosion in a canyon or channel (type 2a) or from a landslide in a canyon (e.g. Montery Canyon, Greene *et al.* 2002), a channel (Turmel *et al.* 2015) or on a slope, such as along the margin of the US East Atlantic coast (Chaytor *et al.*

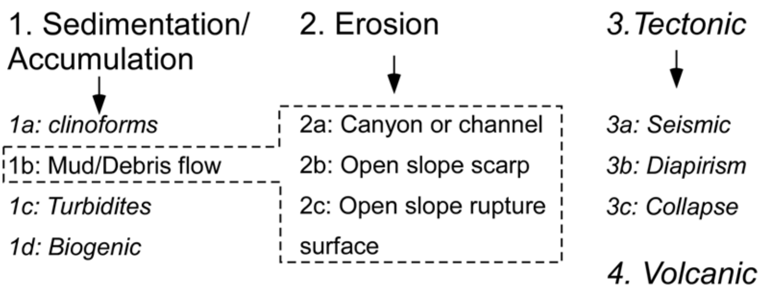

Fig. 6. Classification of slope-forming processes. The processes within the dashed zone are considered as candidates for which the strength can be estimated (see text for explanation).

2009). If a local slope (e.g. clinoform, type 1a) is modified by a landslide, it will show slope scarps (type 2c) and a rupture surface slope (type 2c). Tectonic and volcanic slopes will not be considered here. In the following paragraphs, it is important to remember that the accuracy of the slope morphology will depend on the efficiency of the survey method, for a given depth and geometry of the slopes, to provide adequate spatial resolution.

For the purpose of this paper, the analysis will concentrate on slope types 1b and 2, for which sediment strength estimates are considered possible (within the dashed box in Fig. 6). Slope types 1b and 1c are often associated with mass transport deposits, but imply different physical mechanisms. Type 2 slopes are related to mass wasting process under the term 'eroded slopes'. It has been shown by Locat & Lee (2002) and Locat *et al.* (2010) that eroded slopes (type 2) reflect the intact strength of the material involved in a slide, whereas accumulated slopes (type 1b) composed of debris or mud flow deposits can be related to the remoulded strength (or critical yield strength) of the failed sediments. The analysis of type 1b slopes is much easier when debris or mud flows are exposed. When they are buried, their morphological description may require high-resolution three-dimensional seismic data, as illustrated by Alves (2015).

Hereafter, to follow the order from failure to post-failure, first eroded slopes (type 2) will be considered and then accumulated slopes (type 1b).

Eroded slopes (type 2) and intact strength

Eroded slopes will be considered in two groups: (1) canyons and channels and (2) open slopes. This approach considers that there has been no evolution of the slope morphology since the time of failure, which is certainly not the case in many situations, particularly where there are strong currents that may have brought sediments into the landslide area, as observed in the Gulf of Lions region (Baztan *et al.* 2005; Sultan *et al.* 2007*a*, *b*).

Canyons and channels with continuous erosion (type 2a)

Baztan *et al.* (2005) have shown that canyon incision in canyons of the Western Gulf of Lion is a key process in canyon evolution. In a detailed geotechnical analysis of the Bourcat Canyon, which included *in situ* measurements, Sultan *et al.* (2007*a*, *b*) concluded that: 'Good agreement between present canyon morphology and the shape of the predicted failure surfaces generated by axial incision indicates that axial incision can be one of the main external mechanisms leading to sediment destabilization of inner canyon walls' (Sultan *et al.* 2007*a*, *b*, p. 24). For the Bourcat canyon, the friction angle has been measured to be 30° (Sultan *et al.* 2007*a*, *b*).

Similar observations were made for the Cap de Creus Canyon, to the south, by Sansoucy *et al.* (2007) and Sansoucy (2008). The Cap de Creus slope angles along the flanks can reach values between 20° and 27°. The friction angle obtained from triaxial tests of the sediment is 31° with a cohesion of 3 kPa. This analysis showed that instability can only develop when the incision process approaches the toe of the slope and that it involves relatively thin (<25 m) slope failures with the angle of the rupture surface close to the actual average slope of the flank, i.e. with a slope angle close to the friction angle of the sediment. One of the main observations from these studies of canyons in the western part of the Gulf of Lions is that the continuous erosion of canyons or channels without any sign of large landslides suggests that the slope instability of the canyon flanks occurs under drained conditions and consists mostly of shallow landslides.

The compilation of slope height and slope angle for the Hudson Canyon area presented in Figure 7 shows that the slope angle is between 20° and 30° for actively eroded canyon flanks (Locat *et al.* 2010). This relationship cannot be applied to abandoned canyons or canyons that are being filled because this process only affects the slope height (see Fig. 7). This is the case for the Hudson Canyon

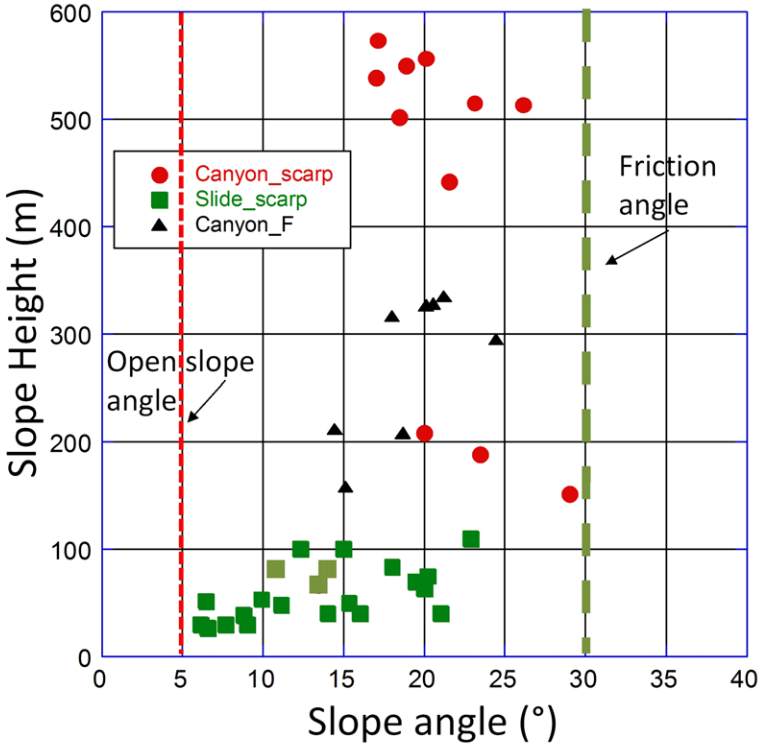

Fig. 7. Compilation of various slope angles and height along the southern New England slope (modified after Locat *et al.* 2010).

shown in Figure 4b. For canyons under active erosion, the slope angle of the canyon walls can be used as a first estimate of the shear strength of the sediment, assuming that FS = 1. The actual slope of the canyon flanks can also vary if the nature of the sediments changes, particularly if bedrock is encountered during the formation of the canyon (Brothers *et al.* 2013; Chaytor *et al.* 2016). Another element to consider is that when canyon incision takes place in clinoforms, the greater steepness of the local canyon wall slopes may also be a result of the fact that the slopes are cut in a direction perpendicular to the inclination of the bed.

Landslide scars on open slopes (types 2b and 2c)

Large submarine landslides have been mapped on both sides of the Atlantic and, in many cases, have developed a rupture surface more or less along a stratigraphic horizon (e.g. the Storegga Slide, Kvalstad *et al.* 2005). On the US Atlantic seaboard, these slides probably developed along clinoform horizons (Chaytor *et al.* 2009). When landslide scars are present, their morphology can be used to assess the shear strength of the sediments prior to failure, assuming that the adjacent slope scarps represent the shear strength characteristics of the intact sediment before failure.

Locat *et al.* (2007) carried out an inventory of the numerous landslide slope scarps and slope rupture surfaces along the southern New England slope. They found that the landslide slope scarp angles (type 2b) varied between 7° and 23° with a slope height from 25 to 110 m, increasing with slope scarp angle (Fig. 7). Similarly, the Currituck Slide to the south (Fig. 8) presents a significant scarp just below a well-defined rupture surface with a height of nearly 750 m and scarp slope angles varying between 15° and 30°. The lower portion of this scarp may be partly cut into Pliocene age sediments (Hill *et al.* 2017). The scarp slope angles reported here are clearly an indication that the sediment strength, prior to failure, was at least equivalent to that of a normally consolidated sediment, so that as a first approximation it could be used to provide a range in mobilized friction angle values for a slope stability analysis under drained conditions.

Figure 7 shows that scarp slopes on the southern New England slope are less than the friction angle.

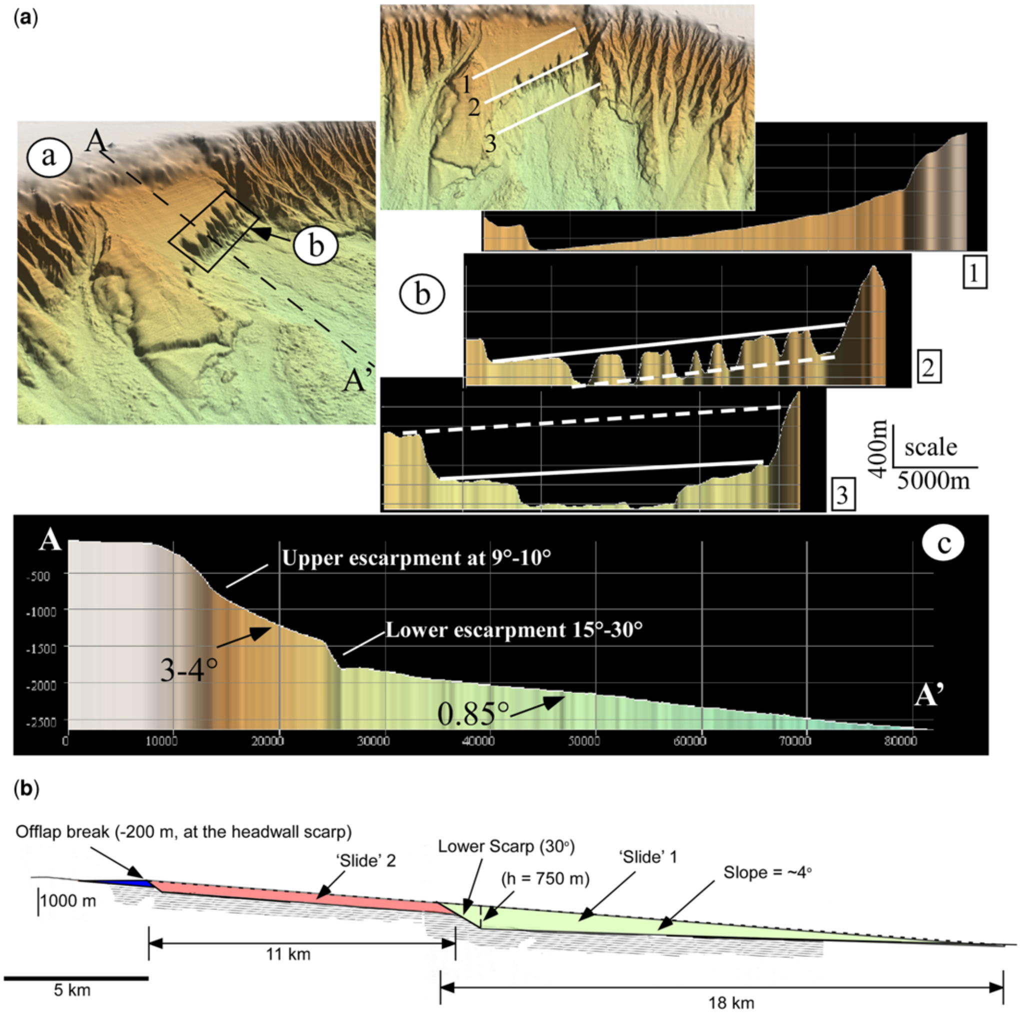

Fig. 8. Topographic views of the Currituck Slide: (**a**) multibeam seismic views with an exaggerated scale (about 12×); and (**b**) cross-section at scale (modified after Locat *et al.* 2009).

Seepage forces do exist along the New Jersey continental slope, as reported by Robb (1984) and Dugan & Flemings (2002). In such a case, the reported values of slope angles for landslide scarp slopes on the southern New England slope could represent the variation of the mobilized friction angle at failure with the existing local excess pore pressures. Conversely, if this approach is valid, and considering the friction angle as a constant parameter, then the value of r_u^+ corresponding to a given slope angle could be used to estimate the *in situ* excess pore pressures.

The rupture surface slopes (type 2c) do not directly provide strength estimates, but they can be used to identify a zone in which sediments are over-consolidated by erosion (Ikari & Kopf 2015; see also Sultan *et al.* 2007*a*, *b* for a detailed analysis of erosion and over-consolidation in a canyon). Estimating the amount of erosion will provide an input to define the variation of strength with depth if any future stability analysis is necessary. For the southern New England slope, Locat *et al.* (2007) reported that the visible rupture surface angles on open slopes varied between 0.3° and 3.0°. For the Currituck Slide (Fig. 8), these angles varied between 3° and 5°. These surfaces appear more or less controlled by the inclination of the bedding planes in both examples.

Rupture surface slope angles must be considered in the analysis of the sliding process. For the Currituck Slide, if we take the actual geometry of the overall rupture surface (*c.* 5°) and carry out a slope stability analysis under either drained or undrained conditions, then the calculated factor of safety will be high if the pore pressure or earthquake triggers are not considered. Routinely (e.g. Masson *et al.* 2006), we should always look at the role of these sources of strength reduction in generating large submarine slides. An earthquake has been favoured as the main trigger for the Currituck Slide (Locat *et al.* 2009), although Hill *et al.* (2017) favour overpressure conditions. The sliding process was such that most of the failed sediments moved down onto the continental rise. This indicates that the available remoulding energy was higher than the energy necessary to reach the remoulded strength of the sediment, although intact blocks are still present in the slide debris.

It is interesting to note that, following the study of the Storegga Slide, greater attention has been paid to the process of progressive failure (Kvalstad *et al.* 2005). Such a process is also favoured in overconsolidated sediments because they can exhibit strain-softening behaviour, which is often one of the conditions for progressive failure to develop and initiate spreading (Leroueil *et al.* 2012). An interesting aspect of the role of progressive failure in slide initiation, which will not be developed here, is that large landslides, like spreads, can form on a flat rupture surface (nearly 0° slope) without the need for a strong external force such as an earthquake or excess pore pressure (Leroueil *et al.* 2012). More research is needed into the role of progressive failure in the development of large submarine slides.

Accumulated slopes (type 1b) and yield strength

Accumulated slopes (type 1b), as defined here, include those formed as a result of debris or mud flows generated by upstream landslides and exclude those formed by turbidity currents. The main morphological elements that can be used for validating the yield strength are the slope angle over which the flow stopped (β), the thickness of the debris in the distal part of the deposit (H_c), corresponding to a single event, and the volume of the debris (V) for the event investigated.

The example of the Pointe-du-Fort Slide will be used here to illustrate this approach; details on the mechanical and physical properties are provided in Locat *et al.* (2007, 2018). This slide is of interest because, unusually, the sediments in the starting zone (tidal flat) and in the deposition zone could also be investigated so that the morphological approach proposed here was better constrained.

The Pointe-du-Fort Slide, located at the entrance of Baie des Ha! Ha! in the Saguenay Fjord, was probably triggered by an earthquake in 1663 (Locat *et al.* 2007). With an estimated volume of 2 Hm^3, the Pointe-du-Fort Slide is to be considered as a small submarine slide, which is seen here as a positive element in simplifying the process of linking the slide source to its deposit. It took place along the shoreline of a tidal flat eroded in marine clay and till (Fig. 9). The topography before failure was reconstructed from the nearby intact slopes. The submarine slope

Fig. 9. Location of the Pointe-du-Fort Slide scarp along the shoreline of the Baie des Ha! Ha! showing the various terraces (from 0 to 100 m) formed as the land emerged. On the tidal flat, the contact is shown between the marine clay and the underlying till (dashed line). The location of borehole BH2 is also shown and is positioned in Figure 10. Image from Google Earth: DigitalGlobe and City of Saguenay 2010.

prior to the slide had an angle of *c.* 24° and a height of 150 m (Fig. 10b). Because the slide was caused by an earthquake, the slope stability analysis was carried out with undrained conditions using a value of $Su/\sigma_{vo} = 0.29$ based on field measurements (Locat *et al.* 2018). As shown in Figure 10c, the failure surface obtained with the minimum factor of safety (FS = 1.8), without earthquake loading, gave a sliding mass with a thickness of *c.* 25 m and a rupture surface length of 480 m. A pseudostatic seismic acceleration coefficient between 0.2 and 0.3 would be sufficient to bring the value of the factor of safety to ≤1 (Urgeles *et al.* 2002; Locat *et al.* 2007).

The slide debris travelled towards the centre of the fjord over a distance of *c.* 1200 m from the crest of the landslide scarp with a run-out angle (*farböschung*, Fig. 10b) of 7.5°. The debris stabilized on a slope of *c.* 1.5° with an average thickness (H_c) of 13 m over a length of 750 m and a width of 300 m for an estimated volume of 1.95 Hm^3, which is similar to the value estimated from slope stability analysis and the scarp morphology (Locat *et al.* 2007).

Tests on samples from both the tidal flat and the debris indicated that the relationship between the remoulded undrained shear strength and the yield strength were similar. Accordingly, the following relationship, consistent with that found by Locat & Demers (1988), was used for the mobility analysis:

$$\tau_c = \left[\frac{Su_r}{1.1}\right]^{1.11} \quad (7)$$

In the debris (core LCF07), the undrained shear strength varied from 1.3 to 5 kPa and equation (6) gives a range of yield strengths from 2.5 to 11.5 kPa. Using H_c (equation 3) gives a range of yield strengths from 1.9 to 2.9 kPa. With a viscosity value of 1 Pa s, BING was used to carry out a parametric analysis to help constrain the yield strength using the position of the front of the debris and the initial thickness (i.e. that of the initial slide volume), which is used for the mobility analysis. The results are shown in Figure 11a using two values for the yield strength: 2000 and 3000 Pa (units required by

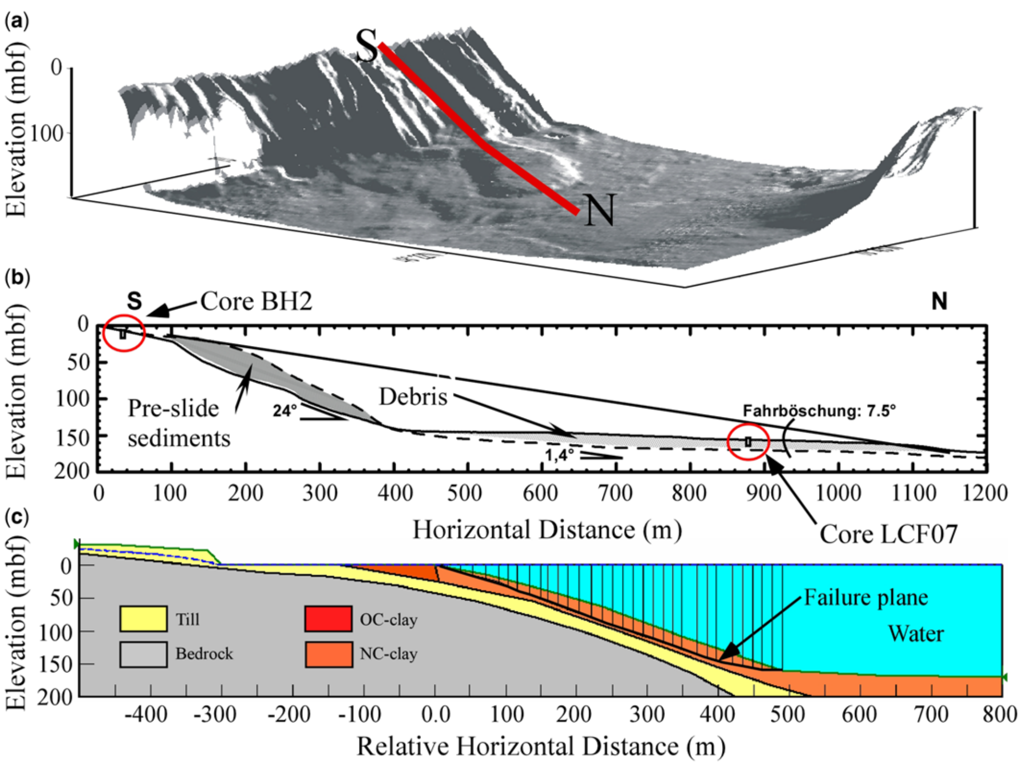

Fig. 10. (**a**) Pointe-du-Fort Slide multibeam three-dimensional morphology. (**b**) Approximate pre-slide conditions and the distribution of the debris showing the location of the referenced boreholes (BH2 and LCF07). (**c**) Geological/geotechnical model used for the slope stability analysis with the Slope/W software (modified after Locat *et al.* 2007). NC, normally consolidated deposit; OC, over-consolidated deposit.

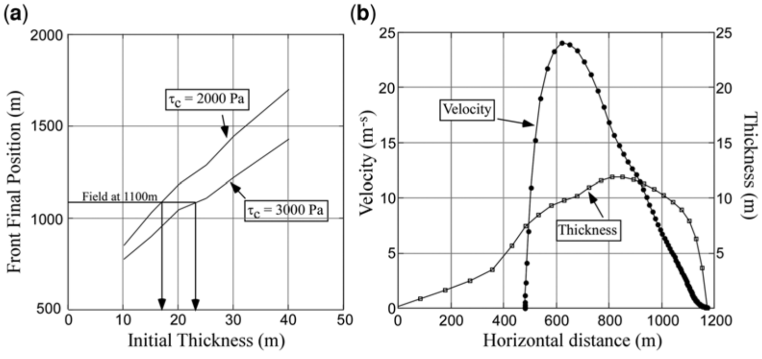

Fig. 11. (**a**) Parametric analysis of the run-out distance as a function of the initial thickness of the slide mass using two values for the yield strength. (**b**) Result of flow modelling using BING for a yield strength of 3000 Pa, giving an estimate of the velocity of the frontal element and the shape of the final deposit (modified after Locat *et al.* 2007).

BING). From this, a yield strength of 3000 Pa (or 3 kPa) was used to model the flow. The flow modelling results are provided in Figure 11b and yield a maximum thickness of *c.* 13 m with an average of *c.* 10 m, still fairly close to the average field value of 13 m. Although the velocity of the frontal element peaked at 25 m s^{-1}, there is no evidence of hydroplaning (e.g. resulting in the detachment of the frontal part of the flow slide), which, according to Mohrig *et al.* (1998), should be possible for velocities >6 m s^{-1}.

A similar study was carried out for the Currituck Slide (Fig. 8) to evaluate whether the two slides were the result of a single event. The mobility analysis was performed using the morphology of the deposit, the run-out distance and the estimated volume of the slides. The conclusion here was that to obtain the observed large run-out distance, the slide had to take place in a single event (Locat *et al.* 2009).

The analyses of the Pointe-du-Fort and Currituck Slides are being used here to show that the morphology of the slide and the resulting debris deposit can be used to constrain the post-failure analysis and that the relationships provided here help in making a first estimate of the post-failure characteristics. For the Pointe-du-Fort Slide, the volume of the slide at failure compares well with the slide deposit. This is not always the case in situations where mass transport deposits or mass transport complexes are identified. In such a case, if these deposits cannot be related to the source, as was also done by Sawyer *et al.* (2009), the interpretation on the initial sliding mechanism may contains too many uncertainties, even more if significant turbidity currents are involved in the process.

Discussion

The geomorphology and geomechanical concepts discussed in this paper could be considered in various ways. Here, the discussion is limited to two points: the timing of excess pore pressure and mass movements involving rock slopes.

Timing of excess pore pressures

Excess pore pressure (or the equivalent if caused by gas expansion) may result from many factors (Dugan & Flemings 2002), including groundwater flow from coastal areas into the continental slopes, the dissociation of gas hydrates (Sultan *et al.* 2004*a*, *b*), consolidation (Prior & Suhayada 1979) and earthquakes (Kvalstad *et al.* 2005). The timing of excess pore pressure relative to the development of the strength of the material and slide initiation is crucial. The Currituck Slide will be used to illustrate this point. Locat *et al.* (2009) concluded that the excess pore pressure due to sediment build-up alone needs to be excessively high to bring the factor of safety to ≤1. Locat *et al.* (2009) estimated that an excess pore pressure of *c.* 1600 kPa was necessary to trigger a failure along the observed rupture surface with a sediment thickness of 200 m. In such a situation, if these pressures were still present, then the actual slope angle of the slide escarpments would be much less. Hill *et al.* (2017), in their detailed review preconditioning factors for the Currituck Slide, argue that the excess pore pressures could be related to the high sedimentation rate during both the late Miocene and Quaternary. If these conditions were the cause of the slide, then why would the slope of the slide escarpments remain stable at an angle of up to 30°? This situation is similar to that observed for the Storegga Slide, where the headwall of the slide has a slope between 20° and 30°. Kvalstad *et al.* (2005) consider that the main reason for the large Storegga landslide is the development of progressive failure, which developed into a large spread failure; this process does not require a high excess pore pressure for its initiation. This does not mean that there was no development of excess pore pressure during the late Miocene sedimentation in the Currituck Slide area, but we need to take this point further and provide pore pressure estimates that support this argument and explain the observed slide and regional morphology.

Rock slopes

This paper focuses on slope developed in sediments (or soils, in the engineering sense). Hungr *et al.* (2013) provide a review of Varne's classification, which includes the nature of the material involved (i.e. rock or soil). This concept (Figure 4) also applies to failures in rock slopes, but involves other geomechanical aspects, such as failure criteria (Locat *et al.* 2000). The vast majority of rock slides are governed by the presence of discontinuities and their characteristics (e.g. roughness, imbrication, bridging), so that the cohesion of the intact rock, which can reach a few MPa, is rarely mobilized in a rock slide (Hoek & Bray 1981). As for sediments, external factors can contribute to instability, such as pore pressures and earthquakes; equation (1) can be used for a back-analysis of a slide if its geometry can be adequately determined (see Schleier *et al.* 2017 for an interesting example).

For the post-failure behaviour of a rock mass, there are many types of mass movement that can also be described using fluid mechanics concepts and rheological parameters (Hungr *et al.* 2013; McDougall 2016). To that effect, in the absence of direct measurements of the rheology of a fluidized rock mass, a submarine rock avalanche can still be modelled rheologically and, in this case, the use of the equation (3) can provide an estimation of the mobilized strength during the flow (Locat *et al.* 2004; Hungr 2006; Sosio *et al.* 2008). León *et al.* (2017) provide an interesting example in which both the source of the rock slide and the various deposits could be matched to constrain the analysis of the failure and post-failure phases of the mass movement.

Concluding remarks

This paper attempts to illustrate how the soil mechanics concepts developed for non-fossiliferous soils can be used to understand and explain the observed slide geomorphology of subaqueous mass movements. Conversely, the morphology of the deposit can be used to validate the rheological parameters necessary for the post-failure analysis of mass movements that can be analysed using fluid mechanics principles. This paper aims to provide help in examples where there is a limited amount of information on the properties of the sediments, the *in situ* conditions and slope processes. The main aspects developed here can be summarized by the following remarks.

(1) The terminology describing the mechanical behaviour of sediments should be consistent with soil mechanics concepts.

(2) In the presence of normally consolidated or over-consolidated sediments, significant excess pore pressures (or their equivalent) in the sediment would probably have been generated after the end of the consolidation process. In such a case, the sedimentation rates associated with the formation of that particular stratigraphic sequence cannot be invoked for the presence of excess pore pressures.

(3) As the slope becomes higher or the failure surface deeper, the contribution of cohesion to the shearing resistance of the sediment decreases significantly, which can be neglected in most cases.

(4) The geometry of slopes resulting from debris or mud flows can be used to assess the strength of the sediment at the time of deposition provided that the initial slide volume can be estimated or the associated thickness (H_c) can be linked to a single event.

(5) In the absence of *in situ* measurements or geotechnical tests on cores, the geometry of the landslide slope scarps and post-failure slope scarps can be used to assess the mobilized shearing resistance (or strength) of the sediment prior to failure.

Acknowledgements This paper benefited from its presentation at the 22nd Laurits Bjerrum Lecture in Oslo, Norway in 2009 and as a Geological Engineering Distinguished Lecturer for the UBC Geological Engineering and the Vancouver Geotechnical Society in Vancouver, Canada in 2015. The author thanks Dominique Turmel, Morelia Urlaub and an anonymous reviewer for their constructive reviews. This paper is a result of the experience acquired with many colleagues around the world. I am very grateful for their friendship and that of Homa Lee in particular.

Funding Funding for this research has been largely provided by the National Science and Research Council of Canada (NSERC).

References

Alves, T.M. 2015. Submarine slide blocks and associated soft-sediment deformation in deep-water basins: a review. *Marine and Petroleum Geology*, **67**, 262–285.

Baztan, J., Berné, S. *et al.* 2005. Axial incision: the key to understanding submarine canyon evolution (in the western Gulf of Lions). *Marine and Petroleum Geology*, **22**, 805–826.

Brothers, D.S., ten Brink, U.S., Andrews, B.D. & Chaytor, J.D. 2013. Geomorphic characterization of the U.S. Atlantic continental margin. *Marine Geology*, **338**, 46–63.

Bünz, S., Mienert, J., Bryn, P. & Berg, K. 2005. Fluid flow impact on slope failure from 3D seismic data: a case study in the Storegga Slide. *Basin Research*, **17**, 109–122.

Chaytor, J.D., ten Brink, A.R., Solow, J. & Andrews, B.D. 2009. Size distribution of submarine landslides along the U.S. Atlantic Margin. *Marine Geology*, **264**, 16–27.

Chaytor, J.D., Demopoulos, A.W.J., ten Brink, U., Baster, C., Quattrini, A.M. & Brothers, D.S. 2016. Assessment of canyon wall failure process from multibeam bathymetry and remotely operated vehicle (ROV) observations, U.S. Atlantic continental margin. *In*: Lamarche, G., Mountjoy, J. *et al.* (eds) *Submarine Mass Movements and their Consequences*. Advances in Natural and Technological Hazards Research, Springer, Switzerland, **41**, 103–113.

Coussot, P. & Piau, J.-M. 1994. On the behavior of fine mud suspensions. *Rheologica Acta*, **33**, 175–184.

De Blasio, F.V., Elverhoi, A., Issler, D., Harbitz, C.B., Bryn, P. & Lien, R. 2005. On the dynamics of subaqueous clay rich gravity mass flows – the giant Storegga slide, Norway. *Marine and Petroleum Geology*, **22**, 179–186.

Dugan, B. & Flemings, P.B. 2002. Fluid flow and stability of the US continental slope offshore New Jersey from Pleistocene to the present. *Geofluids*, **2**, 137–146.

Edgers, L. & Karlsrud, K. 1982. Soil flows generated by submarine slides: case studies and consequences. *In*: Chryssostomomidis, C. & Connor, J.J. (eds) *Proceedings of the 3rd International Conference on the Behavior of Offshore Structures*. Vol. 2. Hemisphere Publishing, Cambridge, 425–437.

Flemings, P.B., Long, H., Dugan, B., Germaine, J., John, C.M., Behrmann, J.H., Sawyer, D. & IODP Expedition 308 scientists 2008. Pore pressure penetrometers document high overpressure near the seafloor where multiple submarine landslides have occurred on the continental slope, offshore Louisiana, Gulf of Mexico. *Earth and Planetary Science Letters*, **269**, 309–325.

Greene, H.G., Maher, N.M. & Paull, C.K. 2002. Physiography of the Monterey Bay national Marine Sanctuary and implications about continental margin development. *Marine Geology*, **181**, 55–82.

Grilli, S.T., Shelby, M. *et al.* 2017. Modeling coastal tsunami hazard from submarine mass failures: effect of slide rheology, experimental validation, and case studies off the US East Coast. *Natural Hazards*, **86**, 353–391.

Grozic, J.L.H. 2010. Interplay between gas hydrates and submarine slope failures. *In*: Mosher, D.C., Shipp, R.C. *et al.* (eds) *Submarine Mass Movements and Their Consequences*. Advances in Natural and Technological Hazards Research, Springer, New York, **28**, 11–30.

Gibson, R.E., England, G.L. & Husseym, J.L. 1967. The theory of one-dimensional consolidation of saturated clays, I. Finite non-linear consolidation of thin homogeneous layers. *Géotechnique*, **17**, 261–273.

Gibson, R.E., Schiffman, R.L. & Cargill, K.W. 1981. The theory of one-dimensional consolidation of saturated clays. II. Finite nonlinear consolidation of thick homogeneous layers. *Canadian Geotechnical Journal*, **18**, 280–293.

Hampton, M.A. 1972. The role of subaqueous debris flows in generating turbidity currents. *Journal of Sedimentary Petrology*, **42**, 775–793.

Hampton, M.A. 1975. Competence of fine debris flows. *Journal of Sedimentary Petrology*, **45**, 834–844.

Hill, J.C., Brothers, D.S., Craig, B.K., ten Brink, U.S., Chaytor, J.D. & Flores, C.H. 2017. Geologic controls on submarine slope failure along the central U.S. Atlantic margin: insights from the Currituck Slide Complex. *Marine Geology*, **385**, 114–130.

Hoek, E & Bray, J. 1981. *Rock Slope Engineering*. 3rd ed. Institute of Mining and Metallurgy, London.

Hutchinson, J.N. 1986. A sliding-consolidation model for flow slides. *Canadian Geotechnical Journal*, **23**, 115–126.

Hutchinson, J.N. 2001. Reading the ground: morphology and site appraisal. *Quarterly Journal of Engineering Geology and Hydrogeology*, **34**, 7–50, https://doi.org/10.1144/qjegh.34.1.7

Hungr, O. 2006. Rock avalanche occurrence, process, and modelling. *In*: Evans, S.G., Magnozza, S.S. *et al.* (eds) *Landslides from Massive Rock Slope Failure*. Springer, Dordrecht, 243–266.

Hungr, O., Leroueil, S. & Picarelli, L. 2013. The Varnes classification of landslides, an update. *Landslides*, **11**, 167–194.

Ikari, M.J. & Kopf, A.J. 2011. Cohesive strength of clay-rich sediment. *Geophysical Research Letters*, **38**, L16309, https://doi.org/10.1029/2011GL047918

Ikari, M.J. & Kopf, A.J. 2015. The role of cohesion and overconsolidation in submarine slope failures. *Marine Geology*, **369**, 153–161.

Imran, J., Parker, G., Locat, J. & Lee, H. 2001. 1D numerical model of muddy subaqueous and subaerial debris flows. *Journal of Hydraulic Engineering*, **127**, 959–968.

Issler, D., De Blasio, F.V., Elverhoi, A., Bryn, P. & Lien, R. 2005. Scaling behaviour of clay-rich submarine debris flows. *Marine and Petroleum Geology*, **22**, 187–194.

Jeong, S.W., Locat, J., Leroueil, S. & Malet, J.-P. 2010. Rheological properties of fine-grained sediment: the role of texture and mineralogy. *Canadian Geotechnical Journal*, **47**, 1085–1100.

Kvalstad, T.T., Andresen, L., Forsberg, C.F., Berg, K., Bryn, P. & Wangen, M. 2005. The Storegga slide: evolution of triggering sources and slide mechanics. *Marine and Petroleum Geology*, **22**, 245–256.

Lee, C., Yun, T.S., Lee, J.-S., Bahk, J.J. & Santamarina, J.C. 2011. Geotechnical characterization of marine sediments in the Ulleung Basin, East Sea. *Engineering Geology*, **117**, 151–158.

Lee, H.J. & Edwards, B.D. 1986. Regional method to assess offshore slope stability. *Journal of Geotechnical Engineering*, **112**, 489–509.

Lee, H.J., Schwab, W.C., Edwards, B.D. & Kayen, R.E. 1991. Quantitative controls on submarine slope failure morphology. *Marine Geotechnology*, **10**, 143–157.

Lee, H.J., Orzech, K., Locat, J., Boulanger, E. & Konrad, J.M. 2004. Seismic strengthening, a conditioning factor influencing submarine landslide development. Paper presented at the 57th Canadian Geotechnical Conference, 2–7 October 2004, Québec City, Canada, 8–14.

Lee, H.J., Locat, J. *et al.* 2007. Submarine mass movements on continental margins. *In*: Nittrouer, C.A., Austin, J.A., Field, M.E., Kravitz, J.H., Syvitski, J.P.M. & Wiberg, P.L. (eds) *Continental Margin Sedimentation: From Sediment Transport to Sequence Stratigraphy*. Blackwell, Oxford, 213–274, https://doi.org/10.1002/9781444304398

Lefebvre, G. 1981. Fourth Canadian Geotechnical Colloquium: strength and slope stability in Canadian soft clay deposits. *Canadian Geotechnical Journal*, **18**, 420–442.

León, R., Somoza, L. *et al.* 2017. Multi-event oceanic island landslides: new onshore–offshore insights from El Hierro Island, Canary Archipelago. *Marine Geology*, **393**, 156–175, https://doi.org/10.1016/j.margeo.2016.07.001

Leroueil, S., Locat, J., Vaunat, J., Picarelli, L., Lee, H. & Faure, R. 1996. Geotechnical characterization of landslides. *In*: Senneset, K. (ed.) *7th International Symposium on Landslides*. Balkerna, Rotterdam, **1**, 53–74.

Leroueil, S., Locat, A., Eberhardt, E. & Kovacevic, N. 2012. Progressive failure in natural and engineered slopes. *In*: Eberhardt, E., Froese, C., Turner, A.K. & Leroueil, S. (eds) *Protecting Society Through Improved Understanding: Proceedings of the 11th International and 2nd North American Symposium on Landslides and Engineered Slopes*, Banff, Canada, 3–8 June 2012. Vol. 1. CRC Press, Boca Raton, FL, 31–46.

Levesque, C., Locat, J. & Leroueil, S. 2006. Dating submarine mass movements triggered by earthquakes in the Upper Saguenay Fjord, Quebec, Canada. *Norwegian Journal of Geology*, **86**, 231–242.

Locat, A., Leroueil, S., Bernander, S., Demers, D., Jostad, H.P. & Ouehb, L. 2011. Progressive failures in eastern Canadian and Scandinavian sensitive clays. *Canadian Geotechnical Journal*, **48**, 1696–1712.

Locat, J. 1997. Normalized rheological behaviour of fine muds and their flow properties in a pseudoplastic regime. *In*: Chen, C.L. (ed). *Proceedings of the 1st International Conference on Debris-Flow Hazards Mitigation*, San Francisco, CA, USA, 260–269.

Locat, J. 2001. Instabilities along ocean margins: a geomorphological and geotechnical perspective. *Marine and Petroleum Geology*, **18**, 503–512.

Locat, J. 2017. Subaqueous mass movements in North America: diversity and issues. *In*: *Proceedings of the 3rd North American Symposium on Landslides*. Association of Environmental & Engineering Geologists, 4–8 June 2017, Roanoke, Virginia, USA, 109–120.

Locat, J. & Demers, D. 1988. Viscosity, remolded strength and liquidity index relationship for high water content soils. *Canadian Geotechnical Journal*, **25**, 799–806.

Locat, J. & Lee, H.A. 2005. Subaqueous debris flows. *In*: Jakob, M. & Hungr, O. (eds) *Debris Flow Hazards and Related Phenomena*. Springer, Dordrecht, 203–245.

Locat, J. & Lee, H.J. 2002. Submarine landslides advances and challenges. *Canadian Geotechnical Journal*, **39**, 193–212.

Locat, J. & Tanaka, H. 2001. A new class of soils: fossilifereous soils. *In*: *Proceedings of the 15th International Conference on Soil Mechanics and Geotechnical Engineering*, 27–31 August 2001, Istanbul, Turkey, Vol. 3. 2295–2300.

Locat, J., Lee, H.J., Nelson, C.H., Schwab, W.C. & Twichell, D.C. 1996. Analysis of the mobility of far reaching debris flows on the Mississippi Fan, Gulf of Mexico. *In*: Senneset, K. (ed.) *Proceedings of the Seventh International Symposium on Landslides,* Trondheim, Norway. Vol. 1. A.A. Balkema, Rotterdam, 555–560.

Locat, J., Picarelli, L. & Leroueil, S. 2000. Some considerations on the role of geological history on slope stability and estimation of the minimum apparent cohesion of a rock mass. *In*: Bromhead, E., Dixon, N. & Ibsen, M.L. (eds) *The 8th International Symposium on Landslides*, 26–30 June 2000, Cardiff, UK, 935–942.

Locat, J., Tanaka, H., Tan, H.S., Dasari, G.R. & Lee, H. 2003. Natural soils: geotechnical behavior and geological knowledge. *In*: Tan, T.S., Phoon, K.K. *et al.* (eds) *Characterisation and Engineering Properties of Natural Soils*. Swets & Zeitlinger, Lisse, 3–28.

Locat, J., Locat, P., Lee, H.J. & Imran, J. 2004. Numerical analysis of the mobility of the Palos Verdes debris avalanche, California, and its implication for the generation of tsunamis. *Marine Geology*, **203**, 269–280.

Locat, J., Locat, P., Locat, A. & Leroueil, S. 2007. Linking geotechnical and rheological properties from failure to post-failure: the Pointe-du-Fort slide, Saguenay Fjord, Québec. *In*: Lykousis, V., Sakellariou, D. & Locat, J. (eds) *Submarine Mass Movements and Their Consequences*, Springer, Dordrecht, 181–189.

Locat, J., Lee, H.J., ten Brink, U.S., Twichell, D., Geist, E. & Sansoucy, M. 2009. Geomorphology, stability and mobility of the Currituck slide. *Marine Geology*, **264**, 28–40.

Locat, J., ten Brink, U. & Chaytor, J.D. 2010. The Block composite submarine landslide, southern New England Slope, U.S.A.: a morphological analysis. *In*: Mosher, D.C. *et al.* (eds) *Submarine Mass Movements and Their Consequences*. Advances in Natural and Technological Hazards Research, **28**, 267–277.

Locat, J., Leroueil, S., Locat, A. & Lee, H. 2014. Weak layers: their definition and classification from a geotechnical perspective. *In*: Krastel, S. *et al.* (eds) *Submarine Mass Movements and Their Consequences*. Advances in Natural and Technological Hazards Research, **37**, 3–12.

Locat, J., Locat, P., Leroueil, S. & Locat, A. 2018. The Pointe-du-Fort case study. *In*: Leroueil, S. & Picarelli, L. (eds) *Understanding Landslides through Case Studies*. Taylor & Francis, Section 8.5.

Longva, O., Janbu, N., Blikra, L.H. & Boe, R. 2003. The 1996 Finneidfjord Slide, seafloor failure and slide dynamics. *In*: Locat, J. & Mienert, J. (eds) *Submarine Mass Movements and Their Consequences*. Kluwer, Dordrecht, 531–538.

Malet, J.P., Remaître, A., Ancey, C., Locat, J., Meunier, M. & Maquaire, O. 2002. Caractérisation rhéologique des coulées de débris et laves torrentielles du bassin marneux de Barcelonnette. Premiers résultats. *Rhéologie*, **1**, 17–25.

Masson, D.G., Harbitz, C.B., Wynn, R.B., Pedersen, G. & Lovholt, F. 2006. Submarine landslides: processes, triggers and hazard prediction. *Philosophical Transactions of the Royal Society*, **364**, 2009–2039.

McDougall, S. 2016. 2014 Canadian Geotechnical Colloquium: landslide runout analysis – current practice and challenges. *Canadian Geotechnical Journal*, **54**, 605–620.

Mesri, G., Ullrich, C.R. & Choi, Y.K. 1978. The rate of swelling of overconsolidated clays subjected to unloading. *Géotechnique*, **28**, 281–307.

Mienert, J., Vanneste, M., Bunz, S., Andreassen, K., Haflidason, H. & Sjrup, H.P. 2005. Ocean warming and gas hydrate stability on the mid-Norwegian margin at the Storegga slide. *Marine and Petroleum Geology*, **22**, 233–244.

Mohrig, D., Whipple, K.X., Hondzo, M., Ellis, C. & Parker, G. 1998. Hydroplaning of subaqueous debris flows. *Geological Society of America Bulletin*, **110**, 387–394.

Mosher, D.C. & Piper, D.J.W. 2007. Analysis of multibeam seafloor imagery of the Laurentian Fan and the 1929 Grand Banks landslide area. *In*: Lykousis, V., Sakellariou, D. & Locat, J. (eds) *Submarine Mass Movements and Their Consequences*, Springer, Dordrecht, 77–88.

Perret, D., Locat, J. & Leroueil, S. 1995. Strength development with burial during early diagenesis in fine grained sediments from Saguenay Fjord, Québec. *Canadian Geotechnical Journal*, **32**, 247–262.

Pittenger, A., Taylor, E. & Bryant, W.R. 1989. The influence of biogenic silica on the geotechnical stratigraphy of the Voring Plateau, Norwegian Sea. *Proceedings of the Ocean Drilling Program, Scientific Results*, **104**, 923–940.

Poulos, H.G. 1988. *Marine Geotechnics*. Unwin Hyman, London.

Prior, D.B. & Suhayada, J.N. 1979. Application of infinite slope analysis to subaqueous sediment instability, Mississippi Delta. *Engineering Geology*, **14**, 1–10.

Qiao, S.F. & Clayton, C.R.I. 2013. Flow slides run-out prediction using a sliding-consolidation model. *Landslides*, **10**, 831–842.

Quiros, G., Young, A.G., Pelletier, J.H. & Chan, J.H.-C. 1983. Shear strength characteristics for Gulf of Mexico clays. *In*: Wright, S.G. (ed.) *Proceedings of the Geotechnical Practice in Offshore Geotechnical Engineering*, ASCE Speciality Conference, 27–28 April, Austin, TX, USA, 144–165.

Rack, F.R., Bryant, W.R. & Julsen, A.P. 1993. Microfabric and physical properties of deep-sea high latitude carbonate oozes. *In*: Rezak, R. & Lavoie, D.L. (eds) *Carbonate Facies*. Springer, New York, 129–147.

Riboulot, V., Cattaneo, A., Sultan, N., Garziglia, S., Ker, S., Imbert, P. & Voisset, M. 2013. Sea level change and free gas occurrence influencing a submarine landslide and pockmark formation and distribution in deepwater Nigeria. *Earth and Planetary Science Letters*, **375**, 78–91.

Robb, J.M. 1984. Spring sapping on the lower continental slope, offshore New Jersey. *Geology*, **12**, 278–282.

Sansoucy, M. 2008. *Analyse de la stabilité des flancs d'un canyon sous-marin, le canyon du Cap de Creus, mer Méditerranée*. MSc thesis, Laval University.

Sansoucy, M., Locat, J. & Lee, H. 2007. Geotechnical considerations of submarine canyon formation: the case of Cap de Creus canyon, Mediterranean Sea. *In*: Lykousis, V., Sakellariu, D. & Locat, J. (eds) *Submarine Mass Movements and Their Consequences*. Advances in Natural and Technological Hazards Research. Springer, Dordrecht, **27**, 181–189.

Saint-Ange, F., Kuus, P., Blasco, S., Piper, J.W., Hughes Clarke, J. & MacKillop, K. 2014. Multiple failure styles related to shallow gas and fluid venting, upper slope Canadian Beaufort Sea, northern Canada. *Marine Geology*, **355**, 136–149.

Sawyer, D.E. & DeVore, J.R. 2015. Elevated strength of sediments on active margins: evidence for seismic strengthening. *Geophysical Research Letters*, **42**, 10.216–10.221.

Sawyer, D.E., Flemings, P.B., Dugan, B. & Germaine, J.T. 2009. Retrogressive failures recorded in mass transport deposits in the Ursa Basin, northern Gulf of Mexico. *Journal of Geophysical Research*, **114**, B10102, https://doi.org/10.1029/2008JB006159

Schleier, M., Hermanns, R.L., Gosse, J.C., Oppikofer, T., Rolm, J. & Tonnesen, J.F. 2017. Subaqueous rock-avalanche deposits exposed by post-glacial isostatic rebound, Innfjorddalen, Western Norway. *Geomorphology*, **289**, 117–133.

Schwab, W.C., Lee, H.J., Twichell, D.C., Locat, J., Nelson, H., McArthur, W.G. & Kenyon, N.H. 1996. Sediment mass-flow processes on a depositional lobe, outer Mississippi Fan. *Journal of Sedimentary Petrology*, **66**, 916–927.

Shephard, L.E., Bryant, W.R. & Dunlap, W.A. 1978. Consolidation characteristics and excess pore pressure of Mississippi Delta sediment. Offshore Technology Conference, 8–11 May 1978, Houston, USA, OTC-3167, 1037–1048, https://doi.org/10.4043/3167-MS

Shiwakoti, D.R., Tanaka, H., Tanaka, M. & Locat, J. 2002. Influence of diatom microfossils on engineering properties of soils. *Soils and Foundations*, **42**, 1–17.

Sosio, R., Crosta, G.B. & Hungr, O. 2008. Complete dynamic modeling calibration for the Thurwieser rock avalanche (Italian Central Alps). *Engineering Geology*, **100**, 11–26.

Steward, T., Sivakugan, N., Shukla, S.K. & Das, B.M. 2011. Taylors's slope stability charts revisited. *International Journal of Geomechanics*, **11**, 348–352.

Sultan, N., Cochonat, P. *et al*. 2004*a*. Triggering mechanisms of slope instability processes and sediment failures on continental margins: a geotechnical approach. *Marine Geology*, **213**, 291–321.

Sultan, N., Cochonat, P., Foucher, J.P. & Mienert, J. 2004*b*. Effect of gas hydrate melting on seafloor slope instability. *Marine Geology*, **213**, 379–401.

Sultan, N., Gaudin, M., Berné, S., Baztan, J., Canals, M., Urgeles, R. & Lafuerza, S. 2007*a*. Analysis of slope failures in submarine canyon heads: an example from the Gulf of Lions. *Journal of Geophysical Research*, **112**, F01009, https://doi.org/10.1029/2005JF000408

Sultan, N., Voisset, M., Marsset, B., Marsset, T.E., Cauquil, E. & Colliat, J.-L. 2007*b*. Potential role of compressional structures in generating submarine slope failures in the Niger Delta. *Marine Geology*, **237**, 169–190.

Talling, P.J., Clare, M., Urlaub, M., Pope, E., Hunt, J.E. & Watt, S.F.L. 2014. Large submarine landslides on continental slopes: geohazards, methane release, and climate change. *Oceanography*, **27**, 32–45.

Tanaka, H. & Locat, J. 1999. A microstructural investigation of Osaka Bay clay: impact of microfossils on its mechanical behaviour. *Canadian Geotechnical Journal*, **36**, 493–508.

Ten Brink, U.S., Andrews, B.D. & Miller, N.C. 2016. Seismicity and sedimentation rate effects on submarine slope stability. *Geology*, **44**, 563–566.

Thakur, V., Degago, S.A. *et al*. 2014. Characterization of post-failure movements of landslides in soft sensitive clays. *In*: L'Heureux, J.-S. *et al*. (eds) *Landslides in Sensitive Clays: From Geosciences to Risk Management*. Advances in Natural and Technological Hazards Research, Springer, New York, **36**, 91–103.

Turmel, D., Locat, J., Locat, P. & Demers, D. 2017. Parametric analysis of the mobility of debris from flow slides in sensitive clays. *In*: Thakur, V., Locat, A. *et al*. (eds) *Landslides in Sensitive Clays*. Advances in Natural and Technological Hazards Research, Springer, New York, **46**, https://doi.org/10.1007/978-3-319-56487-6_27

Turmel, D., Parker, G. & Locat, J. 2015. Evolution of an anthropic source-to-sink system: Wabush Lake. *Earth-Science Reviews*, **151**, 227–243.

Urgeles, R., Locat, J., Lee, H.J. & Martin, F. 2002. The Saguenay Fjord, Canada: integrating marine geotechnical and geophysical data for spatial seismic slope stability and hazard assessment. *Marine Geology*, **185**, 319–340.

Wiemer, G. & Kopf, A. 2017. Influence of diatoms microfossils on sediment strength and slope stability. *Geochemistry, Geophysics, Geosystems*, **18**, 333–345.